Nano World Journal

https://doi.org/10.17756/nwj.2023-s2-076

Research Article

Open Access

Synthesis and Crystal Structure of a New Phosphate $Na_{1.37}Co_{1.36}Cr_{1.64}(PO_4)_3$ with the α-$CrPO_4$ Structure

Sirine El Arni*, Mohammed Hadouchi, Jamal Khmiyas, Abderrazzak Assani, Mohamed Saadi and Lahcen El Ammari

Laboratoire de Chimie Appliquée des Matériaux, Centre des Sciences des Matériaux, Faculty of Science, Mohammed V University in Rabat, Avenue Ibn Battouta, BP 1014, Rabat, Morocco

***Correspondence to:**

Sirine El Arni
Laboratoire de Chimie Appliquée des Matériaux,
Centre des Sciences des Matériaux,
Faculty of Science,
Mohammed V University in Rabat,
Avenue Ibn Battouta, BP 1014,
Rabat, Morocco.
E-mail: sirine.elarni@um5r.ac.ma

Received: July 25, 2023
Accepted: September 27, 2023
Published: September 29, 2023

Citation: El Arni S, Hadouchi M, Khmiyas J, Assani A, Saadi M, et al. 2023. Synthesis and Crystal Structure of a New Phosphate $Na_{1.37}Co_{1.36}Cr_{1.64}(PO_4)_3$ with the α-$CrPO_4$ Structure. *NanoWorld J* 9(S2): S449-S454.

Published by United Scientific Group

Abstract

Phosphate materials have attracted a growing interest for their promising applications such as catalysts and electrode materials. In the context of the elaboration and structural study of novel phosphates, we present in this work a new phosphate, $Na_{1.37}Co_{1.36}Cr_{1.64}(PO_4)_3$, belonging to the well-established structure type, α-$CrPO_4$. This phosphate was produced via a solid-state process and its structure was deduced from single-crystal diffraction data. The $Na_{1.37}Co_{1.36}Cr_{1.64}(PO_4)_3$ crystallizes in orthorhombic symmetry, with the *Imma* space group and unit cell parameters: a = 10.4148(1) Å, b = 13.1091(2) Å, c = 6.4403(1) Å, and V = 879.29 (2) $Å^3$. The framework is made up of PO_4 tetrahedra, $(Cr1/Co1)O_6$ octahedra and $(Co2/Cr2)_2O_{10}$ dimers octahedra. The structure of the title compound can be described as an assembly of two building units: (1) sheets parallel to the (b,c) plane, consisting of the corner and edges sharing $(Co2/Cr2)_2O_{10}$ dimers and $P(2)O_4$ tetrahedra, (2) chains made from corner-sharing $(Cr1/Co1)O_6$ octahedra and $P(1)O_4$ tetrahedra running along the *b*-axis. The association of these building units gives rise to a 3D (Three-dimensional) architecture with two distinct kinds of tunnels parallel to the a and b directions where the Na^+ ions are situated. The Na atoms are both surrounded by eight oxygens.

Keywords

Crystal structure, Solid-state reaction, Three-dimensional framework, α-$CrPO_4$-type structure

Introduction

Mixed alkali and transition metal phosphates with tunnel and layered structures have received much attention and have been explored in several research areas such as magnetism [1, 2]. Indeed, the inclusion of transition metals within the structure results in exceptional magnetic properties, like ferromagnetic [3], antiferromagnetic [4, 5] or ferrimagnetic [6, 7] behavior, in addition to their possible applicability as electrode materials for batteries [8, 9]. Owing to their high structural stability, several transition metal phosphates with a 3D architecture have undergone in-depth research. Among the well-known families of those materials, we can cite, Alluaudite [10], α-$CrPO_4$ [11], NASICON [12], and Olivine [13, 14].

In fact, out of the various categories of phosphates, one of our areas of focus is centered on tunnel-type structures [15, 16]. These materials have shown their usefulness in a diverse range of applications as catalysts, anticorrosive pigments, sensors, or materials used to manufacture lasers [17-19]. For instance, a significant research effort has been reported on the α-$CrPO_4$-type structure. This type of structure is effectively used in electrode materials due to the large channels available for alkali-ion migration, for instance, $NaCoCr_2(PO_4)_3$, $NaNiCr_2(PO_4)_3$,

and $Na_2Ni_2Cr(PO_4)_3$ were tested as anodes in Na-ion batteries and it has been shown that these compounds delivered high specific capacities [11]. Moreover, α-VPO_4 has been investigated as an effective anode component for Na-ion batteries [20].

During our investigation of the $A_2O/MO/P_2O_5$, seeking new materials with open structures likely to exhibit exciting properties, many new crystalline compounds with diverse structures and belonging to distinct chemical classes have been identified, namely, α-$CrPO_4$-type structure. In the same framework, our research team has synthesized and characterized new transition metals-based materials belonging to this type of structure, such as $MNi_2Fe(PO_4)_3$ (M = Ca and Sr) [21, 22], $MCo_2Fe(PO_4)_3$ (M = Ba and Sr) [23, 24], $MMn^{II}{}_2Mn^{III}(PO_4)_3$ (M = Ba, Sr, and Pb) [25-27].

To further enrich this specific area of research, the present work introduces the elaboration and structural characterization of a new non-stoichiometric phosphate $Na_{1.37}Co_{1.36}Cr_{1.64}(PO_4)_3$ exhibiting the α-$CrPO_4$ structure.

Materials and Methode

Single crystals synthesis

The phosphate $Na_{1.37}Co_{1.36}Cr_{1.64}(PO_4)_3$ was synthesized through a solid-state reaction, with the reactants consisting of $NaNO_3$ (≥ 99%, Merck), $(CH_3COO)_2Co.4H_2O$ (≥ 99%, Merck), Cr $(NO_3)_3.9H_2O$ (≥ 98%, Merck), and $NH_4H_2PO_4$ (≥ 99.6%, Acros Organics) in the molar ratio of Na:Co:Cr:P = 2:2:1:3. This mixture was dissolved in an aqueous solution containing a few drops of HNO_3, stirred continuously for two hours on a magnetic stirrer and then air-dried overnight on a hot plate to evaporate the water. The collected powder was then transferred to a platinum crucible and heated in a furnace. The temperature was raised to 1343 K, where melting occurs, and held for two hours before being cooled to 1143 K at a rate of 5 K/h. Dark brown crystals of an appropriate size were found for the X-ray diffraction (XRD) study.

Structure determination

An appropriate single crystal was placed on a thin glass fiber on a Bruker D8 Venture Super DUO diffractometer with PHOTON100 CMOS area-detector and monochromatic MoKα radiation (λ = 0.71073 Å) for the data acquisition. The data collection was gathered using the APEX3 program [28] and the absorption correction was carried out by a multi-scan semi-empirical approach using SADABS [29]. The direct method was used to solve the crystal structure, while SHELXT 2013 and SHELXL 2013 were used for refinement [30, 31]. These programs are implemented in the WinGX software package [32]. In order to create the structural graphics, DIAMOND software was used [33]. The structure is determined at nanometric scale.

Results and Discussion

The $Na_{1.37}Co_{1.36}Cr_{1.64}(PO_4)_3$ crystallizes with the well-known α-$CrPO_4$ structure in the *Imma* space group and the unit cell parameters: a = 10.4148(1) Å, b = 13.1091(2) Å, c = 6.4403(1) Å, V = 879.29 (2) Å^3, and Z = 4. Besides O1 and O2 oxygen atoms which are located in general positions, all remaining atoms are located in special positions of the *Imma* space group. Indeed, the Cr and Co atoms share the 4*a* and 8*g* special positions with Cr^{3+}/Co^{2+} occupancy fractions of 0.828/0.172 and 0.406/0.594, respectively. Moreover, the phosphorus atoms occupy 8*g* and 4*e* Wyckoff positions of the *Imma* space group. The sodium atoms are in the 4*b* and 4*e* special positions, the 4*b* site is partially occupied by 36.8% of Na1, while the 4*e* site is fully filled by Na2. The principal crystallographic parameters, atomic positions, and anisotropic displacement parameters for each atom are presented in table 1, table 2, and table 3, respectively. The Bond Valence Sum (BVS) calculations are given in table 2. The BVS values calculated for Cr1 and Cr2 atoms are higher than the BVS values of Co1 and Co2 atoms, which is consistent with the expected oxidation state of Co^{2+} and Cr^{3+} ions. Not that the BVS values of Co atoms are slightly higher than expected which can be explained by site disorder. Moreover, the BVS calculations indicate that the values of P and Na atoms closely align with the anticipated formal total valences of +5 and +1, respectively. Additionally, the BVS values determined for all oxygen atoms are within the expected range of 1.83 - 2.08.

Figure 1a shows the environments of the mixed sites Cr1/Co1 and Co2/Cr2, as well as P and Na atoms. The (Cr1/Co1)O_6 octahedron shows a moderate distortion as the Cr1/Co1—O distances range from 1.9745 (7) Å to 2.0400 (12) Å. Similarly, the cationic disorder causes a strong deformation of the (Co2/Cr2)O_6 as illustrated in figure 1a. The Co2/Cr2—O distances vary between 2.0414 (8) Å and 2.0609 (7) Å. The

Table 1: Crystal data, data collection, and refinement structure details of $Na_{1.37}Co_{1.36}Cr_{1.64}(PO_4)_3$.

Crystal data	
Chemical formula	$Na_{1.37}Co_{1.36}Cr_{1.64}(PO_4)_3$
M_r (g/mol)	481.64
Crystal system, space group	Orthorhombic, *Imma*
a, b, *c* (Å)	10.4148 (1), 13.1091 (2), 6.4403 (1)
V (Å^3)	879.29 (2)
Z	4
μ (mm^{-1})	5.21
Data collection	
Diffractometer	Bruker D8 Venture
Absorption correction	Multi-scan (SADABS; [29])
No. of measured, independent and observed [I> 2σ(I)] reflections	18003, 1462, 1382
R_{int}	0.029
θ_{min} - θ_{max} (°)	3.1- 40.0
Temperature (K)	296
Radiation type	X-ray, Mo Kα radiation (λ = 0.71073Å)
Refinement	
$R[F^2 > 2s(F^2)]$, $wR(F^2)$, *S*	0.019, 0.055, 1.11
No. of reflections	1462
No. of parameters	60
$\Delta\rho_{max}$, $\Delta\rho_{min}$ (e Å^{-3})	1.21, -0.72

Table 2: Fractional atomic coordinates, equivalent isotropic displacement parameters (Å²), and BVS for $Na_{1.37}Co_{1.36}Cr_{1.64}(PO_4)_3$.

	Wyck.	*x*	*y*	*z*	U_{eq}	Occ. (≤ 1)	BVS
Cr1	*4a*	0.5000	0.5000	0.5000	0.00514 (6)	0.828 (13)	2.884 (3)
Co1	*4a*	0.5000	0.5000	0.5000	0.00514 (6)	0.172 (13)	2.645(3)
Co2	*8g*	0.7500	0.63485 (2)	0.7500	0.00551 (5)	0.594 (12)	2.294 (2)
Cr2	*8g*	0.7500	0.63485 (2)	0.7500	0.00551 (5)	0.406 (12)	2.501(2)
P1	*8g*	0.7500	0.42747 (3)	0.7500	0.00520 (8)	1	4.856(5)
P2	*4e*	1.0000	0.7500	0.91635 (8)	0.00485 (9)	1	4.956(8)
Na1	*4b*	1.0000	0.5000	0.5000	0.0314 (11)	0.368	1.113(1)
Na2	*4e*	1.0000	0.7500	1.4029 (3)	0.0571 (6)	1	0.776(1)
O1	*16j*	0.78634 (9)	0.36528 (6)	0.56147 (13)	0.01115 (14)	1	1.845(3)
O2	*16j*	0.86197 (7)	0.50675 (6)	0.79028 (12)	0.00732 (12)	1	2.060(3)
O3	*8i*	0.88141 (11)	0.7500	0.76930 (17)	0.01008 (18)	1	2.082(4)
O4	*8h*	1.0000	0.65381 (9)	1.0481 (2)	0.01117 (18)	1	1.833(5)

Table 3: Anisotropic displacement parameters (Å²) of all atoms.

	U^{11}	U^{22}	U^{33}	U^{12}	U^{13}	U^{23}
Cr1	0.00349 (10)	0.00509 (11)	0.00683 (11)	0.000	0.000	−0.00144 (8)
Co1	0.00349 (10)	0.00509 (11)	0.00683 (11)	0.000	0.000	−0.00144 (8)
Co2	0.00500 (8)	0.00531 (8)	0.00621 (9)	0.000	−0.00067 (5)	0.000
Cr2	0.00500 (8)	0.00531 (8)	0.00621 (9)	0.000	−0.00067 (5)	0.000
P1	0.00591 (13)	0.00491 (13)	0.00478 (14)	0.000	−0.00002 (9)	0.000
P2	0.00375 (16)	0.00537 (17)	0.00544 (18)	0.000	0.000	0.000
Na1	0.0048 (10)	0.088 (3)	0.0016 (10)	0.000	0.000	−0.0052 (14)
Na2	0.0568 (12)	0.0989 (19)	0.0155 (7)	0.000	0.000	0.000
O1	0.0151 (3)	0.0101 (3)	0.0083 (3)	0.0031 (2)	0.0008 (3)	−0.0029 (2)
O2	0.0063 (2)	0.0075 (2)	0.0081 (3)	−0.0007 (2)	−0.0012 (2)	0.0009 (2)
O3	0.0072 (4)	0.0139 (4)	0.0091 (4)	0.000	−0.0034 (3)	0.000
O4	0.0099 (4)	0.0095 (4)	0.0141 (5)	0.000	0.000	0.0058 (3)

phosphorus atoms adopt tetrahedral environment. The framework of the phosphate $Na_{1.37}Co_{1.36}Cr_{1.64}(PO_4)_3$ can be shown as a 3D assembly of PO_4 tetrahedra, $(Cr1/Co1)O_6$ octahedra and $(Co2/Cr2)_2O_{10}$ dimer units of edge-sharing $(Co2/Cr2)O_6$ octahedra. As seen in figure 1c, these dimer units create sheets parallel to the (b,c) plane by sharing corners and edges with $P(2)O_4$ tetrahedra. Adjacent sheets are bridged to each other through infinite chains of corner sharing $(Cr1/Co1)O_6$ octahedra and $P(1)O_4$ tetrahedra running along the b-axis (Figure 1b). The sheets and chains are joined together to construct an open three-dimensional structure displaying two different kinds of tunnels parallel to [100] and [010] directions where the sodium atoms are positioned as in figure 1d. The Na^+ cations are both surrounded by eight oxygens (Figure 1a). The Na1—O distances are in the range of 2.3599 (8)- 2.8683 (9) Å, whereas the Na2—O bond length varies between 2.610 (2) and 2.6995 (8) Å. The structure of the title compound resembles that of $NaCoCr_2(PO_4)_3$ and $Na_2Ni_2Cr(PO_4)_3$ with two types of sodium atoms in the tunnels [11]. The selected interatomic distances and angles are gathered in table 4.

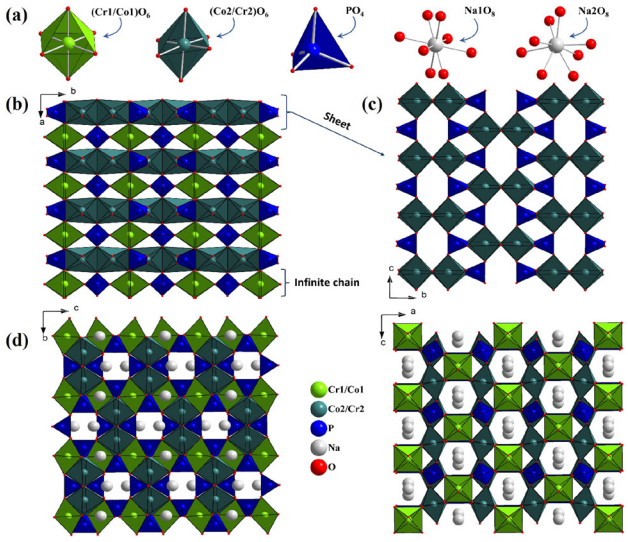

Figure 1: (a) The environments of Cr/Co, P, and Na atoms, **(b)** $[Co_{1.36}Cr_{1.64}(PO_4)_3]_\infty$ framework, **(c)** sheet of edge and corner-sharing $(Co2/Cr2)_2O_{10}$ units and PO_4 tetrahedra parallel to the (b,c) plane, and **(d)** polyhedral representation of the tridimensional framework showing Na^+ cations in two distinct kinds of channels running parallel to [100] and [010] directions.

Conclusion

In summary, single crystals of $Na_{1.37}Co_{1.36}Cr_{1.64}(PO_4)_3$

Table 4: Main interatomic distances (Å) and angles (°) in $Na_{1.37}Co_{1.36}Cr_{1.64}(PO_4)_3$.

Atom				
Cr1/Co1	Distances (Å) Cr1/Co1—O			
	Cr1/Co1—$O2^{i}$	1.9745 (7)	Cr1/Co1—$O2^{iv}$	1.9745 (7)
	Cr1/Co1—$O2^{ii}$	1.9745 (7)	Cr1/Co1—$O4^{iii}$	2.0400 (12)
	Cr1/Co1—$O2^{iii}$	1.9745 (7)	Cr1/Co1—$O4^{iv}$	2.0400(12)
Cr1/Co1	Angles (°) O—Cr1/Co1—O			
	$O2^{i}$—Cr1/Co1—$O2^{ii}$	180.0	$O2^{iii}$—Cr1/Co1—$O4^{iii}$	93.42 (3)
	$O2^{i}$—Cr1/Co1—$O2^{iii}$	86.55 (4)	$O2^{iv}$—Cr1/Co1—$O4^{iii}$	86.58 (3)
	$O2^{ii}$—Cr1/Co1—$O2^{iii}$	93.45 (4)	$O2^{i}$—Cr1/Co1—$O4^{iv}$	93.42 (3)
	$O2^{i}$—Cr1/Co1—$O2^{iv}$	93.45 (4)	$O2^{ii}$—Cr1/Co1—$O4^{iv}$	86.58 (3)
	$O2^{ii}$—Cr1/Co1—$O2^{iv}$	86.55 (4)	$O2^{iii}$—Cr1/Co1—$O4^{iv}$	86.58 (3)
	$O2^{iii}$—Cr1/Co1—$O2^{iv}$	180.0	$O2^{iv}$—Cr1/Co1—$O4^{iv}$	93.42 (3)
	$O2^{i}$—Cr1/Co1—$O4^{iii}$	86.58 (3)	$O4^{iii}$—Cr1/Co1—$O4^{iv}$	180.0
	$O2^{ii}$—Cr1/Co1—$O4^{iii}$	93.42 (3)		
Co2/Cr2	Distances (Å) Co2/Cr2—O			
	Co2/Cr2—O3	2.0414 (8)	Co2/Cr2—$O3^{vii}$	2.0414 (8)
	Co2/Cr2—$O1^{vi}$	2.0414 (8)	Co2/Cr2—O2	2.0608 (7)
	Co2/Cr2—$O1^{v}$	2.0414 (8)	Co2/Cr2—$O2^{ii}$	2.0609 (7)
Co2/Cr2	Angles (°) O—Co2/Cr2—O			
	O3—Co2/Cr2—$O1^{vi}$	86.34 (4)	$O1^{v}$—Co2/Cr2—O2	88.89 (3)
	O3—Co2/Cr2—$O1^{v}$	93.73 (4)	$O3^{vii}$—Co2/Cr2—O2	171.72 (3)
	$O1^{vi}$—Co2/Cr2—$O1^{v}$	179.91 (5)	O3—Co2/Cr2—$O2^{ii}$	171.72 (3)
	O3—Co2/Cr2—$O3^{vii}$	84.63 (5)	$O1^{vi}$—Co2/Cr2—$O2^{ii}$	88.89 (3)
	$O1^{vi}$—Co2/Cr2—$O3^{vii}$	93.73 (4)	$O1^{v}$—Co2/Cr2—$O2^{ii}$	91.04 (3)
	$O1^{v}$—Co2/Cr2—$O3^{vii}$	86.34 (4)	$O3^{vii}$—Co2/Cr2—$O2^{ii}$	102.44 (3)
	O3—Co2/Cr2—O2	102.44 (3)	O2—Co2/Cr2—$O2^{ii}$	70.86 (4)
	$O1^{vi}$—Co2/Cr2—O2	91.04 (3)		
P1	Distances (Å) P1—O			
	P1—O1	1.5107 (8)	P1—$O1^{ii}$	1.5107 (8)
	P1—$O2^{ii}$	1.5835 (7)	P1—O2	1.5835 (7)
P1	Angles (°) O—P1—O			
	O1—P1—$O1^{ii}$	114.68 (7)	O1—P1—O2	107.54 (4)
	O1—P1—$O2^{ii}$	114.02 (4)	$O1^{ii}$—P1—O2	114.02 (4)
	$O1^{ii}$—P1—$O2^{ii}$	107.54 (4)	$O2^{ii}$—P1—O2	97.95 (6)
P2	Distances (Å) P2—O			
	P2—O4	1.5200 (11)	P2—$O3^{viii}$	1.5563 (11)
	P2—$O4^{viii}$	1.5200 (12)	P2—O3	1.5563 (11)
P2	Angles (°) O—P2—O			
	O4—P2—$O4^{viii}$	112.11 (10)	O4—P2—O3	109.86 (3)
	O4—P2—$O3^{viii}$	109.86 (3)	$O4^{viii}$—P2—O3	109.86 (3)
	$O4^{viii}$ —P2—$O3^{viii}$	109.86 (3)	$O3^{viii}$ —P2—O3	105.04 (9)
Na1	Distances (Å) Na1—O			
	Na1—O2	2.3599 (8)	Na1—O1	2.8683 (9)
	Na1—$O2^{x}$	2.3599 (8)	Na1—$O1^{xi}$	2.8683 (9)
	Na1—$O2^{vi}$	2.3599 (8)	Na1—$O1^{x}$	2.8683 (9)
	Na1—$O2^{xi}$	2.3599 (8)	Na1—$O1^{vi}$	2.8683 (9)
Na2	Distances (Å) Na2—O			
	Na2—O4	2.610 (2)	Na2—$O1^{xv}$	2.6995 (9)
	Na2—$O4^{viii}$	2.610 (2)	Na2—$O1^{xvi}$	2.6995 (9)
	Na2—$O3^{xiii}$	2.664 (2)	Na2—$O1^{xvii}$	2.6995 (9)
	Na2—$O3^{xiv}$	2.664 (2)	Na2—$O1^{xviii}$	2.6995 (8)

Note: Symmetry codes: (i) x−1/2, −y+1, z−1/2; (ii) −x+3/2, y, −z+3/2; (iii) x−1/2, y, −z+3/2; (iv) −x+3/2, −y+1, z−1/2; (v) −x+3/2, −y+1, z+1/2; (vi) x, −y+1, −z+1; (vii) −x+3/2, −y+3/2, −z+3/2; (viii) −x+2, −y+3/2, z; (ix) x, y, z−1; (x) −x+2, y, z; (xi) −x+2, −y+1, −z+1; (xii) x+1/2, y, −z+3/2; (xiii) −x+2, −y+3/2, z+1; (xiv) x, y, z+1; (xv) −x+2, y+1/2, −z+2; (xvi) x, −y+1, −z+2; (xvii) −x+2, −y+1, −z+2; (xviii) x, y+1/2, −z+2.

were successfully grown using solid state method and identified structurally through single-crystal XRD data. This phosphate crystallizes with the α-$CrPO_4$-type structure, the latter consists of $[(Co2/Cr2)_2O_{10}]$ dimer units sharing corners and edges with $P(2)O_4$ tetrahedra to create sheets parallel to the (b,c) plane. These sheets are associated together by infinite chains of corner sharing $[(Cr1/Co1)O_6]$ octahedra and $P(1)O_4$ tetrahedra to construct a 3D framework including channels where the sodium atoms are situated.

Acknowledgements

The authors express their heartfelt gratitude to the Faculty of Science, Mohammed V University in Rabat for generously providing X-ray measurements.

Conflict of Interest

The authors affirm that they do not possess any known competing financial interests or personal relationships that may have had an impact on the work reported in this paper.

Funding

The CNRST's Excellence Research Scholarships Program provided funding for this research.

References

1. Souiwa K, Hidouri M, Toulemonde O, Duttine M, Amara MB. 2015. Synthesis and characterization of the phosphates $Na_{1+x}Mg_{1+x}Cr_{2-x}(PO_4)_3$ (x = 0; 0.2) and $NaZnCr_2(PO_4)_3$ with the α-$CrPO_4$ structure. *J Alloys Compd* 627: 153-160. https://doi.org/10.1016/j.jallcom.2014.12.002
2. Benhsina E, Hermouche L, Assani A, Saadi M, Labjar N, et al. 2021. Synthesis, characterization, magnetic properties, and lead sensing based on a new alluaudite-like phosphate $Na_2Mn_2Cr(PO_4)_3$. *J Mater Sci* 56: 2163-2175. https://doi.org/10.1007/s10853-020-05371-2
3. Wright AJ, Ruiz-Valero C, Attfield JP. 1999. Weak ferromagnetism and framework switching in $KMnHP_3O_{10}$. *J Solid State Chem* 145(2): 479-483. https://doi.org/10.1006/jssc.1999.8167
4. Hadouchi M, Assani A, Saadi M, Saadoune I, Lahmar A, et al. 2018. Synthesis, crystal structure and properties of a new phosphate, $Na_2Co_2Cr(PO_4)_3$. *J Inorg Organomet Polym Mater* 28: 2854-2864. https://doi.org/10.1007/s10904-018-0956-y
5. Hadouchi M, Assani A, Saadi M, Kopelevich Y, da Silva RR, et al. 2019. Unconventional spin-glass-like state in $AgCo_2V_3O_{10}$, the novel magnetically frustrated material. *J Magn Magn Mater* 491: 165623. https://doi.org/10.1016/j.jmmm.2019.165623
6. El Arni S, Hadouchi M, Assani A, Saadi M, Lahmar A, et al. 2022. A novel phosphate, $K_4NiFe_3(PO_4)_5$: synthesis, crystal structure and magnetic properties. *J Solid State Chem* 313: 123333. https://doi.org/10.1016/j.jssc.2022.123333
7. Hadouchi M, Assani A, Saadi M, Lahmar A, El Marssi M, et al. 2019. Magnetic properties of a new cobalt hydrogen vanadate with a dumortierite-like structure: $Co_{13.5}(OH)_6(H_{0.5}VO_{3.5})_2(VO_4)_6$. *Acta Cryst Sec C Struct Chem* 75(6): 777-782. https://doi.org/10.1107/S2053229619007186
8. Harbaoui D, Sanad MM, Rossignol C, Amdouni N, Zaidat K, et al. 2022. Effect of divalent transition metal ions on physical, morphological, electrical and electrochemical properties of alluaudite phases $Na_2M^{2+}{}_2Fe^{3+}(PO_4)_3$ (M = Mn, Co and Ni): cathode materials for sodium-ions batteries. *J Alloys Compd* 901: 163641. https://doi.org/10.1016/j.jallcom.2022.163641
9. Essehli R, Belharouak I, Yahia HB, Chamoun R, Orayech B, et al. 2015. α-$Na_2Ni_2Fe(PO_4)_3$: a dual positive/negative electrode material for sodium ion batteries. *Dalt Trans* 44(10): 4526-4532. https://doi.org/10.1039/c5dt00021a
10. Bouftila NEH, Naji M, Ababou Y, Rjeb A, Sayouri S. 2021. Low temperature treatment and structural characterization of $Na_2M_2Fe(PO_4)_3$ (M = Mn or Ni) Alluaudite phases. *IOP Conf Ser Mater Sci Eng* 1160(1): 012004. https://doi.org/10.1088/1757-899X/1160/1/012004
11. Yahia HB, Essehli R, Avdeev M, Park JB, Sun YK, et al. 2016. Neutron diffraction studies of the Na-ion battery electrode materials $NaCoCr_2(PO_4)_3$, $NaNiCr_2(PO_4)_3$, and $Na_2Ni_2Cr(PO_4)_3$. *J Solid State Chem* 238: 103-108. https://doi.org/10.1016/j.jssc.2016.03.011
12. Zhang J, Liu Y, Zhao X, He L, Liu H, et al. 2020. A novel NASICON-type $Na_4MnCr(PO_4)_3$ demonstrating the energy density record of phosphate cathodes for sodium-ion batteries. *Adv Mater* 32(11): 1906348. https://doi.org/10.1002/adma.201906348
13. Liu Y, Wang H, Lin D, Liu C, Hsu PC, et al. 2015. Electrochemical tuning of olivine-type lithium transition-metal phosphates as efficient water oxidation catalysts. *Energy Environ Sci* 8(6): 1719-1724. https://doi.org/10.1039/c5ee01290b
14. Hadouchi M, Koketsu T, Hu Z, Ma J. 2022. The origin of fast-charging lithium iron phosphate for batteries. *Battery Energy* 1(1): 20210010. https://doi.org/10.1002/bte2.20210010
15. Hadouchi M, Assani A, Saadi M, Lahmar A, El Marssi M, et al. 2019. Synthesis, characterization, and magnetic properties of $A_2Co_2Fe(VO_4)_3$ (A = Ag or Na) alluaudite-type vanadates. *J Supercond Nov Magn* 32: 2437-2446. https://doi.org/10.1007/s10948-018-4964-5
16. Lamsakhar NEH, Hadouchi M, Zriouil M, Assani A, Saadi M, et al. 2019. A novel alluaudite-type vanadate, $Na_2Zn_2Fe(VO_4)_3$: synthesis, crystal structure, characterization and magnetic properties. *Inorg Chem Commun* 107: 107472. https://doi.org/10.1016/j.inoche.2019.107472
17. Xu S, Pan D, Wu Y, Song X, Gao L, et al. 2018. Efficient production of furfural from xylose and wheat straw by bifunctional chromium phosphate catalyst in biphasic systems. *Fuel Process Technol* 175: 90-96. https://doi.org/10.1016/j.fuproc.2018.04.005
18. Attfield JP, Battle PD, Cheetham AK. 1985. The spiral magnetic structure of β-chromium(III) orthophosphate (β-$CrPO_4$). *J Solid State Chem* 57(3): 357-361. https://doi.org/10.1016/0022-4596(85)90199-9
19. Apostolescu N, Cernătescu C, Cobzaru C, Tătaru-Fărmuș RE, Vizitiu MA, et al. 2020. Recent advances in anticorrosive phosphate pigments. *Bull Inst Politehnic Din Iași* 66(70): 1-14.
20. Fedotov SS, Samarin AS, Nikitina VA, Stevenson KJ, Abakumov AM, et al. 2019. α-VPO_4: a novel many monovalent ion intercalation anode material for metal-ion batteries. *ACS Appl Mater Interfaces* 11(13): 12431-12440. https://doi.org/10.1021/acsami.8b21272
21. Ouaatta S, Assani A, Saadi M, El Ammari L. 2015. Crystal structure of strontium dinickel iron orthophosphate. *Acta Cryst Sec E Cryst Commun* 71(10): 1255-1258. https://doi.org/10.1107/S205698901501779X
22. Ouaatta S, Assani A, Saadi M, El Ammari L. 2017. Crystal structure of calcium dinickel(II) iron(III) tris(orthophosphate): $CaNi_2Fe(PO_4)_3$. *Acta Cryst Sec E Cryst Commun* 73(6): 893-895. https://doi.org/10.1107/S2056989017007411
23. Bouraima A, Anguile JJ, Assani A, Saadi M, Makani T, et al. 2019. Crystal structure of baryum dicobalt iron(III) three(orthophosphate) belonging to α-$CrPO_4$ family. *Open J Inorg Chem* 10(1): 1-5. https://doi.org/10.4236/ojic.2020.101001
24. Bouraima A, Makani T, Assani A, Saadi M, El Ammari L. 2016. Crystal structure of strontium dicobalt iron(III) tris(orthophosphate): $SrCo_2Fe(PO_4)_3$. *Acta Cryst Sec E Cryst Commun* 72(8): 1143-1146. https://doi.org/10.1107/S2056989016011373
25. Alhakmi G, Assani A, Saadi M, Follet C, El Ammari L. 2013. $SrMn^{II}{}_2Mn^{III}(PO_4)_3$. *Acta Cryst Sec E Cryst Commun* 69: i56. https://doi.org/10.1107/S1600536813020977

26. Assani A, Saadi M, Alhakmi G, Houmadi E, El Ammari L. 2013. $BaMn^{II}_2Mn^{III}(PO_4)_3$. *Acta Cryst Sec E Cryst Commun* 69: i60. https://doi.org/10.1107/S1600536813023106

27. Alhakmi G, Assani A, Saadi M, El Ammari L. 2013. A new mixed-valence lead(II) manganese(II/III) phosphate(V): $PbMn^{II}_2Mn^{III}(PO_4)_3$. *Acta Cryst Sec E Cryst Commun* 69: i40. https://doi.org/10.1107/S1600536813016504

28. Bruker SAINT-Plus. 2012. Bruker AXS Inc., Madison, Wisconsin, USA.

29. Krause L, Herbst-Irmer R, Sheldrick GM, Stalke D. 2015. Comparison of silver and molybdenum microfocus X-ray sources for single-crystal structure determination. *J Appl Cryst* 48(1): 3-10. https://doi.org/10.1107/S1600576714022985

30. Sheldrick GM. 2015. SHELXT-Integrated space-group and crystal-structure determination. *Acta Cryst Sec A Found Adv* 71(1): 3-8. https://doi.org/10.1107/S2053273314026370

31. Sheldrick GM. 2015. Crystal structure refinement with SHELXL. *Acta Cryst Sec C Struct Chem* 71(1): 3-8. https://doi.org/10.1107/S2053229614024218

32. Farrugia LJ. 2012. WinGX and ORTEP for Windows: an update. *J Appl Cryst* 45(4): 849-854. https://doi.org/10.1107/S0021889812029111

33. Putz H, Brandenburg K. 2018. Diamond-Crystal and Molecular Structure Visualization. Crystal Impact-GbR, Kreuzherrenstr. 102, 53227 Bonn, Germany.